Venkatagiriyappa *et al.*
Journal of Engineering and Applied Science (2023) 70:127
https://doi.org/10.1186/s44147-023-00296-4

Journal of Engineering and Applied Science

RESEARCH Open Access

Development of a model for a walking robot made of Desai mechanism using ANN and regression approach

Raghavendra Bommanahalli Venkatagiriyappa[1*], Anandkumar R. Annigeri[1] and Jogipalya Shivananjappa Srikantamurthy[1]

*Correspondence: bvrjss@gmail.com

[1] Department of Mechanical Engineering, JSS Academy of Technical Education, Bengaluru 560060, India

Abstract

The study focuses on computing the optimized foot profile for a walking leg mechanism using artificial neural network (ANN), genetic algorithm, and regression approaches. The technique adopted in this work is the benchmark approach and acts as a tool for complex problems. A mathematical model using regression and ANN is developed for the 8-link coplanar mechanism. Optimum link lengths are obtained to minimize the objective function (error). The output response is the foot length with a minimum foot height of 124 mm for obstacle clearance. A neural network is designed with seven neurons (one neuron/link) in the input layer. Optimum neurons in the hidden layer are determined based on the output obtained through simulation. A single neuron is used to represent the foot profile length at the output layer. The foot lengths obtained from the regression model and ANN are compared and validated with a genetic algorithm for the data sets of 100, 200, 300, 400, and 500. Simulation studies of the walking leg mechanism revealed a difference of 19%, 22.4%, and 5.23% in the foot profile by ANN and mathematical, ANN and regression model, and mathematical and regression approach respectively. This paper reveals that different approaches viz., ANN, mathematical and regression models generate dissimilar foot profiles.

Keywords: Walking leg robot, Artificial neural network, Planar mechanism, Regression model

Introduction

Walking robots mimicking the gait of humans have inspired many researchers in the recent past. Controlling a biped walking mechanism is a complex multivariable problem due to the system's nonlinearity, high dimensionality, and intrinsic instability. In every realistic instance, the exact dynamic equations of a walking robot are either too complicated or impossible to formulate in closed form for use in control solutions. Different types of gait are used by animals in mobility, crawling uphill or downhill, slowly or quickly [1]. Of the various mechanisms developed, the coplanar single-degree-of-freedom mechanism has advantages over other mechanisms. Artificial Intelligence (AI)

enables computers or inanimate objects based on computers to think and act in the same way that people do. Kousik et al. [2] conducted the motion studies of a quadruped robot made of Desai's walking mechanism on a straight path and staircase climbing using SAM 6.1 and SOLIDWORKS software. The stride length and stride height are the parameters of importance in the foot profile of walking mechanisms.

ANN applications have grown tremendously since the mid-twentieth century and are constantly emerging. Oh et al. [3] developed the artificial neural network model to study the effect of ground reaction forces on human gait and fuzzy-controlled humanoid robots are studied [4]. A Neuro-Simulation for complex robots using the bootstrapped method by Woodford and du Plessis [5] and Hexapod walking robots with artificial intelligence capabilities using the ANN approach is studied by Kessis et al. [6]. Authors [7, 8] used neural networks and wavelet methods to analyze the analytical techniques for gait data.

The ANN has been successfully implemented in biomechanical research [9] and in animating human figures while standing, walking, and running [10]. The optimization techniques [11], e.g., genetic algorithm (GA), particle swarm optimization (PSO), artificial bee colony (ABC), backtracking search algorithm (BSA), lightning search algorithm (LSA) and whale optimization algorithm (WOA), were reviewed extensively. Identifying gait-cycle phases is crucial [12] for controlling the walking mechanism, as most humanoid robots walk unhuman-likely with bent knees [13]. The walking fatigue of bipedal robots with compliant feet [14] and the kinematic model of the walking robots for discontinuous contact with the ground [15] were analyzed.

Optimization situations frequently necessitate good algorithms to minimize or maximize objective functions. Gheorghita and Gheorghita [16] optimized a 6-link planar mechanism to develop a regression model using computer software and validated the results experimentally. By a genetic algorithm model, authors [17] synthesized a planar mechanism using regression deviation and converged regression error to a global minimum. Researchers [18] developed an approach combining analytical and statistical methods for studying robot kinematics to reduce the tracking error. Authors [19] developed regression equations for the bipedal walking model and measured ground reaction forces.

Many researchers and industries are interested in developing legged walking robots that resemble humanoid motion [20]. Legged devices replicating legged animals' morphology are useful for movements in off-road travel, including sandy or wet natural areas and space exploration. The benefits of legged mobility vary depending on the posture, number of legs, and leg functionality [21]. An 8-link single *dof* leg mechanism for a walking robot is designed for an optimum stride path and stride height and analyzed different configurations of mechanisms by Desai et al. [22]. The studies of a passive walking biped robot with flexible legs [23] and a coplanar 8-link walking leg mechanism using GA [24] are reported in the literature. The design of experiments concept is used for processes to find the optimum process parameters [25–28]. In optimizing linkage mechanisms, these techniques limit foot profile for both stride length and stride height. Researchers used optimization algorithms in renewable energy, as in comparative analysis of renewable energy sources[29], performance analysis of photovoltaic systems [30, 31], optimal economic indices [32], optimization of PID controller [33], generation of hybrid renewable

power [34], experimental investigation of DC converters [35], hybrid EV studies [36], performance analysis of photovoltaic grid [37], studies on hybrid photovoltaic [38].

In the open literature, regression and ANN models on the performance of a single dof coplanar 8-link walking mechanism are unavailable; hence, this paper attempts to develop regression and ANN models for the Desai mechanism [22] walking robot. This work will be a benchmark study for developing an efficient mathematical model for optimization studies.

Mathematical model for foot profile generation

Walking leg robots generate a foot profile. The coordinates of joints and paths of the links are computed using the principle of the intersection of two circles to find the position of joints in the mechanism for angular rotation of the input crank (L1).

Figure 1 shows the C-2 configuration of the Desai mechanism [22]; Ro is a fixed joint, input link L1 rotates (θ) through 2π radians, and link L1 is formed between joint Ro and joint R1 (in Fig. 1), Ro is fixed joint P, R1 is joint Q, R2 is joint U, R3 is fixed joint S, R4 is joint T). In the Cartesian coordinate system, the Instantaneous position of joint R1(Qx, Qy) can be computed using (1) and (2).

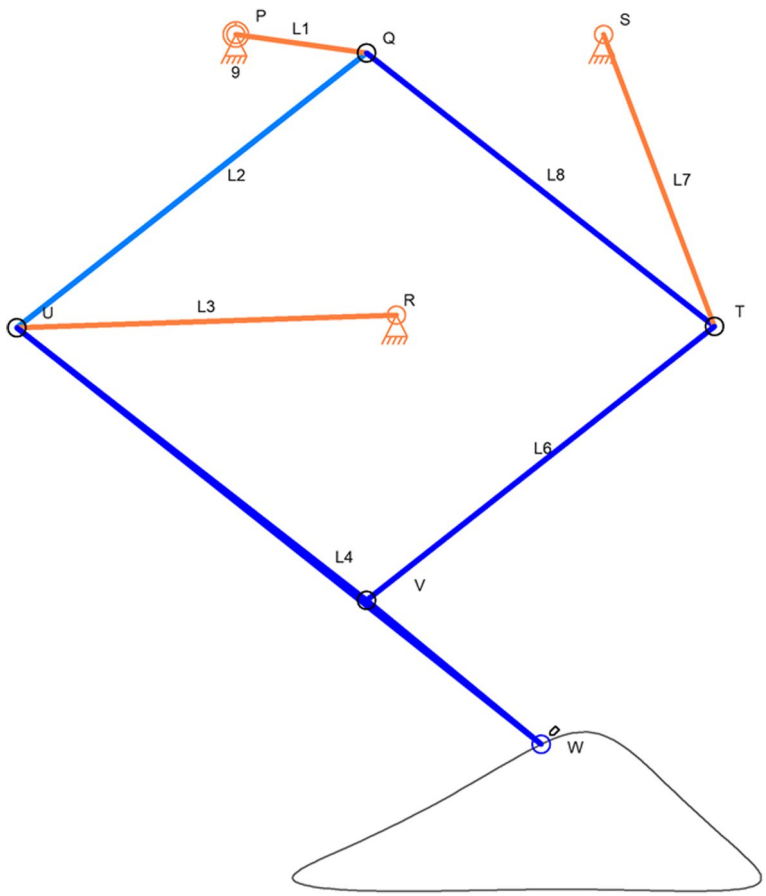

Fig. 1 Kinematic analysis of C-2 configuration [22]

$$\mathrm{Qx} = \mathrm{L1}\ \mathrm{Cos}\theta \tag{1}$$

$$\mathrm{Qy} = \mathrm{L1}\ \mathrm{Sin}\theta \tag{2}$$

The instantaneous coordinates of joint R2(Ux, Uy) are computed using the principle of intersection of circles. R2 is represented as joint U. The two circles with centers R1(Qx, Qy) and R2(Ux, Uy) with radii L2 and L3 respectively, can be expressed as

$$(x - Q_x)^2 + (y - Q_y)^2 = L_2^2 \tag{3}$$

$$(x - R_x)^2 + (y - R_y)^2 = L_3^2 \tag{4}$$

The distance between the centers of two circles with radii R1 and R2 is

$$D_{R_1R_2} = \sqrt{(Q_x - R_x)^2 + (Q_y - R_y)^2} \tag{5}$$

Coordinates of R2 can be expressed as

$$R_{2x_1} or R_{2x_2} = \left(\frac{Q_x + R_x}{2}\right) + \left(\frac{(R_x - Q_x)\left(L_2^2 - L_3^2\right)}{2D_{R_1R_2}^2}\right) \pm 2\Delta\left(\frac{Q_y - R_y}{D_{R_1R}^2}\right) \tag{6}$$

$$R_{2y_1} or R_{2y_2} = \left(\frac{Q_y + R_y}{2}\right) + \left(\frac{\left(R_y - Q_y\right)\left(L_2^2 - L_3^2\right)}{2D_{R_1R_2}^2}\right) \mp 2\Delta\left(\frac{Q_x - R_x}{D_{R_1R_2}^2}\right) \tag{7}$$

$$\Delta = \frac{1}{4}\sqrt{\begin{matrix}\left(D_{R_1R_2} + L_2 + L_3\right)\left(D_{R_1R_2} + L_2 - L_3\right) \\ \left(D_{R_1R_2} - L_2 + L_3\right)\left(-D_{R_1R_2} + L_2 + L_3\right)\end{matrix}} \tag{8}$$

Similarly, the coordinates of joint R4 (Tx, Ty) can be computed as the intersection point of two circles with centers R1(Qx, Qy) and R3(Sx, Sy) with radii L8 and L7, respectively.

$$(x - Q_x)^2 + (y - Q_y)^2 = L_8^2 \tag{9}$$

$$(x - S_x)^2 + (y - S_y)^2 = L_7^2 \tag{10}$$

The distance between two circle centers, R1 and R3, is

$$D_{R_1R_3} = \sqrt{(Q_x - S_x)^2 + (Q_y - S_y)^2} \tag{11}$$

Coordinates of R4 can be expressed as

$$R_{4x_1} or R_{4x_2} = \left(\frac{Q_x + S_x}{2}\right) + \left(\frac{(S_x - Q)\left(L_8^2 - L_7^2\right)}{2D_{R_1R_3}^2}\right) \pm 2\Delta\left(\frac{Q_y - S_y}{D_{R_1R_3}^2}\right) \tag{12}$$

$$R_{4y_1} or R_{4y_2} = \left(\frac{Q_y + S_y}{2}\right) + \left(\frac{(S_y - Q_y)(L_8^2 - L_7^2)}{2D_{R_1R_3}^2}\right) \mp 2\Delta\left(\frac{Q_x - S_x}{D_{R_1R}^2}\right) \tag{13}$$

$$\Delta = \frac{1}{4}\sqrt{\frac{(D_{R_1R_3} + L_8 + L_7)(D_{R_1R_3} + L_8 - L_7)}{(D_{R_1R_3} - L_8 + L_7)(-D_{R_1R} + L_8 + L_7)}} \tag{14}$$

Similarly, the coordinates of joint V (Vx, Vy) are computed as the intersection point of two circles with centers R2(Ux, Uy) and R4(Tx, Ty) with radii L4 and L6, respectively.

$$(x - T_x)^2 + (y - T_y)^2 = L_4^2 \tag{15}$$

$$(x - U_x)^2 + (y - U_y)^2 = L_6^2 \tag{16}$$

Distance between two circle centers, R2 and R4:

$$D_{R_2R_4} = \sqrt{(x - T_x)^2 + (y - T_y)^2} \tag{17}$$

Coordinates of V can be expressed as,

$$V_{x_1} or V_{x_2} = \left(\frac{T_x + U_x}{2}\right) + \left(\frac{(T_x - U_x)(L_4^2 - L_6^2)}{2D_{R_1R_4}^2}\right) \pm 2\Delta\left(\frac{T_y - U_y}{D_{R_1R_4}^2}\right) \tag{18}$$

$$V_{y_1} or V_{y_2} = \left(\frac{T_y + U_y}{2}\right) + \left(\frac{(T_y - U_y)(L_4^2 - L_6^2)}{2D_{R_1R_4}^2}\right) \mp 2\Delta\left(\frac{T_x - U_x}{D_{R_1R_4}^2}\right) \tag{19}$$

$$\Delta = \frac{1}{4}\sqrt{\frac{(D_{R_2R_4} + L_4 + L_6)(D_{R_2R_4} + L_4 - L_6)}{(D_{R_2R_4} - L_4 + L_6)(-D_{R_2R_4} + L_4 + L_6)}} \tag{20}$$

W represents the foot of the walking robot and its slope is the same as that of link L4.

Many researchers have studied the various approaches to minimize the error of the designed six target points and the corresponding points obtained through the fitness candidate. In their study, the best fitness candidate value in the population is the lowest error in the population. A population is an array of the upper and lower bound of all the link lengths 600 mm and 100 mm, respectively, except for input link L1. The stride length and stride height of the foot trajectory of the walking leg mechanism are treated as constraints with a minimum stride length of 300 mm and maximum stride height of 124 mm. For the study, the input link (L1) length is 100 mm and six selected target points on the foot trajectory are

$$\left[W^i{}_{XT}\, W^i{}_{YT}\right] = [(45, -650), (181, -650), (249, -650), (317, -650), (385, -650)]$$

Minimizing the error in the traced path by the foot of the walking robot is the objective per rotation of the input crank. The objective function in the optimization study is given by (21),

$$\text{Minimize} \sum_{i=1}^{N=6} [(W^i{}_{XT} - W^i{}_X)^2 - (W^i{}_{YT} - W^i{}_Y)^2] \tag{21}$$

Six target points ($W^i{}_{XT}, W^i{}_{YT}$)on the foot profile are considered in the objective function for minimization of the error($W^i{}_X, W^i{}_Y$). The ten different constraints are used in the optimization algorithm. Equations (22–25) are used due to Grashof's criteria, as the mechanism comprises two crank rockers (PQUR and PQTS) for smooth leg movement in the stride phase.

$$L_1 + L_2 \leq L_3 + L_{10} \tag{22}$$

$$L_1 + L_8 \leq L_7 + L_9 \tag{23}$$

Here, L1 and L2 represent the shortest and the longest links, with L3 and L10, are other links in polygon PQUR, as in Fig. 1. Similarly, L1 and L8 represent the shortest and longest links, with L7 and L9 being the links in polygon PQTS (Fig. 3a).

$$L_1 \leq \min\{L_2, L_3, L_{10}\} \tag{24}$$

$$L_1 \leq \min\{L_7, L_8, L_9\} \tag{25}$$

Equations (26–27) are the constraints due to the transmission angle of the crank rocker PQUR and PQTS of the mechanism.

$$(\theta_2 - \theta_6) \geq 35^o \tag{26}$$

$$(\theta_5 - \theta_7) \geq 35^o \tag{27}$$

The linkages L2- L4 -L6 -L8 form a parallelogram with the following constraint.

$$\text{L2} = \text{L4} = \text{L6} = \text{L8} \tag{28}$$

Equation (29) lists the constraint on the range of links as Min(Li) = 100 mm and Max(Li) = 600 mm as mechanism design parameters.

$$L \in [Min(L_i), Max(L_i)] \tag{29}$$

The constraint of stride height of the foot in the foot profile is given by (30), with the maximum stride height of the foot being limited to 124 mm.

$$W^i{}_Y \leq W^i{}_Y Max \tag{30}$$

$$W^i{}_X \geq W^i{}_X Min \tag{31}$$

Equation (31) is the constraint on the stride length of the foot for a minimum value of 300 mm.

Methods

In this section, the regression model and ANN models were developed based on the normalized data.

Normalized input data

Simulations were conducted on the 8-link coplanar Desai mechanism [22]. The length of the L_1 is fixed to 100 mm and the location of the three pivot points is also fixed. The lengths of links 2 to 7 (input data) were randomly generated to obtain the foot profile using a mathematical model with a constraint of a minimum foot profile length of 124 mm. The trials were conducted for the sample sizes of 100, 200, 300, 400, and 500. The output of the foot profile length of these samples and found that the foot profile follows a normal distribution (i.e., bell-shaped curve).

Development of regression model

The input and output data from the above trials were used in Minitab software to obtain the regression model. The regression model is further tested with randomly generated link lengths (links 2–7).

The results obtained from the regression model and the mathematical model were compared for various trained data samples.

Development of the ANN model

Input and output data obtained from the above mathematical approach were used for training in ANN. An ANN was designed to take these trials of seven input parameters for link length and angle to obtain output as foot profile length. Randomly generated initial weights are used to train and test the data. All the data of 7-link lengths were given at the input neuron and the output neuron represents foot length in mm; net architecture was created with a hidden layer between the input and output layer. Simulations were conducted to decide the number of neurons in the hidden layer to obtain better output. The neuron in the hidden layer was varied between 1 and 20 and tested for mean square error. The best-simulated trail for the optimum neuron in the hidden layer is selected based on the minimum mean square error.

Seventy percent of the samples were used to train the model, and the remaining 30% were used to validate the model. The minimum coefficient of determination for training data and validation is more than 95% and 91%, respectively. The weights and bias of the best simulation results were extracted. The trained model is further tested with randomly generated link length. The result obtained from the ANN-trained model for randomly generated link length and the mathematical model compared various trained data of samples such as 100, 200, 300, 400, and 500.

Results and discussion

The working of a single degree of freedom 8-link co-planar walking mechanism is analyzed using three approaches. The study highlights the stability of the mechanism during the stride phase and the lift phase with an emphasis on getting a symmetric

bell-shaped foot profile. This section is arranged in three subsections, viz., regression model, ANN, and mathematical model.

Regression model

The regression equation obtained for the horizontal length of the foot profile = $425–0.0382(L_2)$-$0.749(L_3) + 0.371(L_5)$-$0.946(L_7) + 4.08(\text{Theta}) + 0.961(L_8)$-$0.118(\text{TZ})$.

ANN structure with 07 normalized link lengths as input neurons produces foot profile length as outputs. The network is trained with an extensive data set for efficient learning to establish a relationship between inputs and output. The trained network predicts the output by providing randomly generated input (link length) and obtaining the output (foot profile length). The number of neurons in the hidden layers is varied until a satisfactory performance is obtained. The structure of ANN architecture is listed in Table 1. MATLAB Toolbox™ of Neural Network used in the study.

Simulation and testing

After training the ANN using five sets of data (each with 100, 200, 300, 400, and 500 samples). The ANN model and the mathematical model results were compared for foot profile length.

Table 1 Structure of ANN

Number of input neurons	07
Number of hidden layers	01
Number of neurons in a hidden layer	Optimized (18)
Transfer function of hidden layers	Tan-sigmoid
Number of output neuron	01
Transfer function of output neurons	Purelin
Training function	Trainlm
Network performance function	Mse

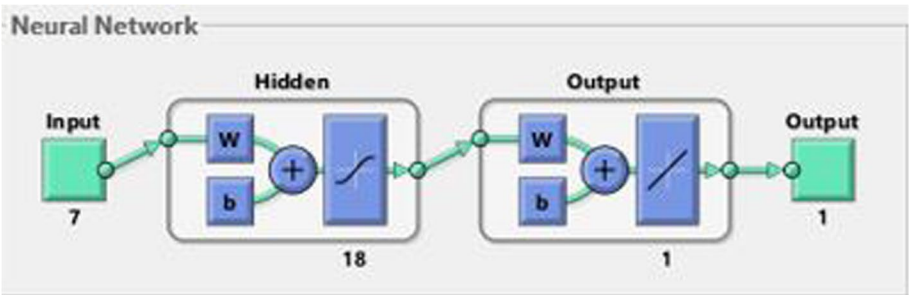

Fig. 2 ANN architecture

Table 2 Weights and bias (generated from the ANN)

Neurons in hidden layer	Weight W1/ Neurons							Bias	Weight W2	Bias
	1	2	3	4	5	6	7			
1	−2.66	−1.85	0.57	−0.10	0.47	−0.98	3.71	2.1	1.06	-0.38
2	0.01	−0.26	−0.93	0.8	−0.36	−0.89	0.97	−2.08	−0.37	
3	−0.04	−0.18	−0.74	−0.79	0.28	−1.77	1.06	−1.10	1.57	
4	−2.76	−0.66	−0.33	−0.08	0.37	0.28	2.51	1.49	−1.23	
5	−1.82	3.03	−1.92	2.22	−0.13	−0.44	0.27	1.7	1.56	
6	0.04	0.86	−1.23	2.55	−0.40	0.36	−1.32	0.48	1.45	
7	−0.43	−0.32	0.83	1.54	1.68	−0.71	−1.43	0.37	−0.30	
8	−1.29	−0.04	−0.78	0.98	0.55	−0.04	2.51	0.1	3.23	
9	−1.80	−2.26	0.08	−2.76	−0.54	−2.50	−1.34	−0.93	0.29	
10	−2.07	−1.36	−0.33	−1.65	0.64	2.02	3.72	−0.40	−2.61	
11	−0.89	1.77	0.48	−0.09	−1.10	−0.58	0.03	−0.34	−0.48	
12	−0.22	3.63	−1.11	2.97	−0.35	−1.20	−4.75	−2.82	−1.16	
13	0.79	1	1.73	1.32	0.29	0.58	−0.52	2.04	0.91	
14	1.64	−1.15	2.6	−2.10	0.18	−0.11	1.63	1.64	0.37	
15	−2.09	0.95	−1.49	−1.24	0.56	1.11	1.89	0.13	−1.24	
16	−1.70	0.52	−0.36	0.4	−0.20	1.34	−0.39	−1.45	0.26	
17	1.64	−0.18	1.94	1.12	0.02	−1.26	−1.18	−2.39	1.59	
18	−0.01	0.84	1.32	−0.07	−1.11	−1.31	1.39	−2.88	0.89	

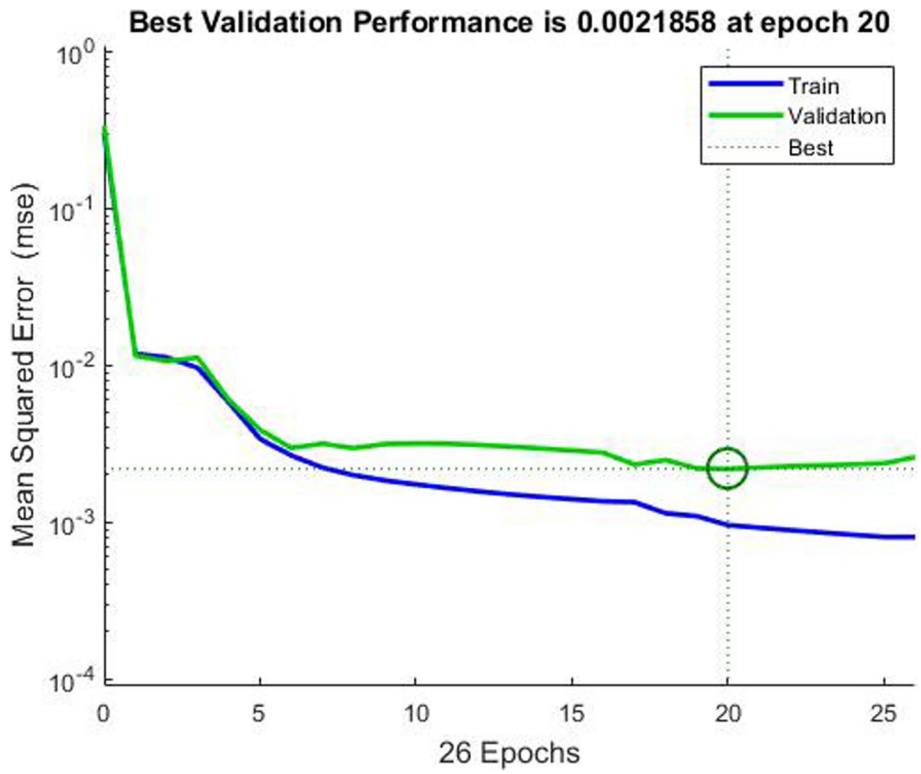

Fig. 3 ANN validation and test

Details for 500 sample data set

Figure 2 shows the architecture of the ANN. Table 2 lists the output obtained after ANN training. Figures 3, 4, 5, 6, and 7 depict the output of ANN.

Architecture of ANN

Foot profile generated using a mathematical model for randomly generated link lengths

The data in Table 3 is used to obtain the foot profile for the Desai mechanism [22]. The GA results for test sets 1, 2, 3, 6, 7, and 11 are used. Figures 8, 9, 10, 11, 12, and 13 show the typical foot profile obtained using the randomly generated link lengths.

The summarised results of foot profiles obtained by ANN, GA, and regression approaches are in Table 4.

The present study has used three approaches, namely GA, ANN, and regression method for optimizing stride length in the foot profile of the 8-link coplanar walking leg Desai mechanism [22]. The results of the GA approach used in this study agree with Raghavendra and Annigeri [24]. The regression model is compared with GA and ANN models and found that they disagree.

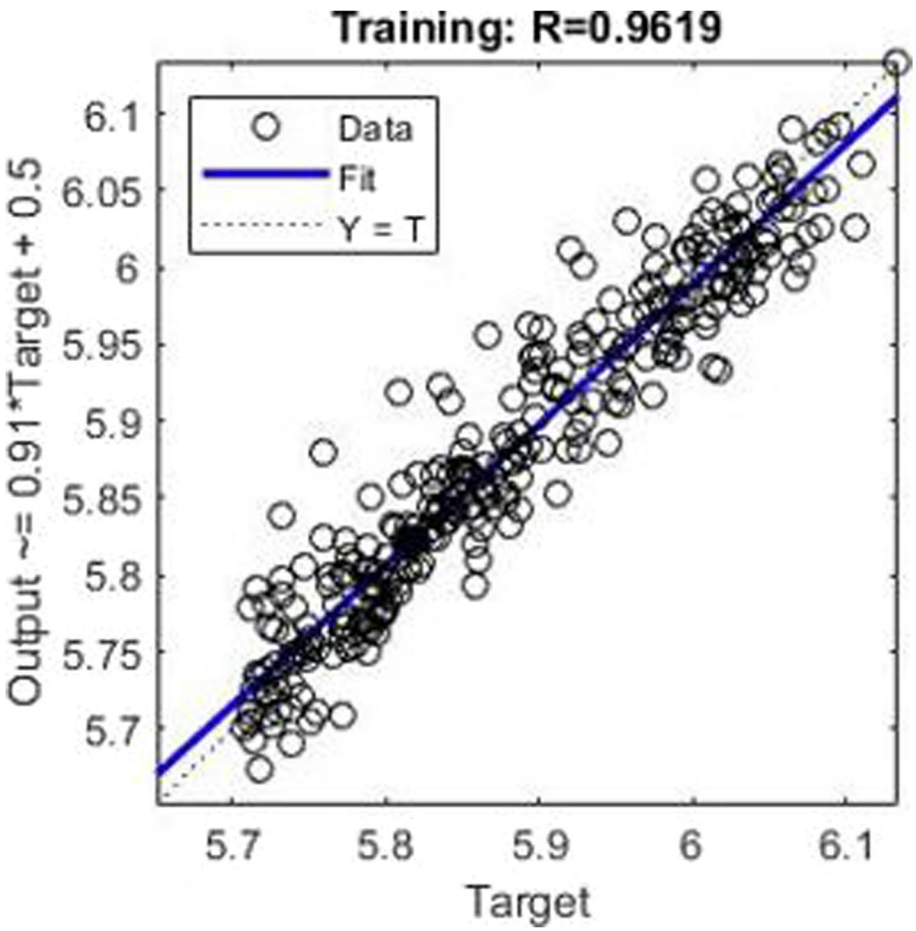

Fig. 4 *R* value (training data)

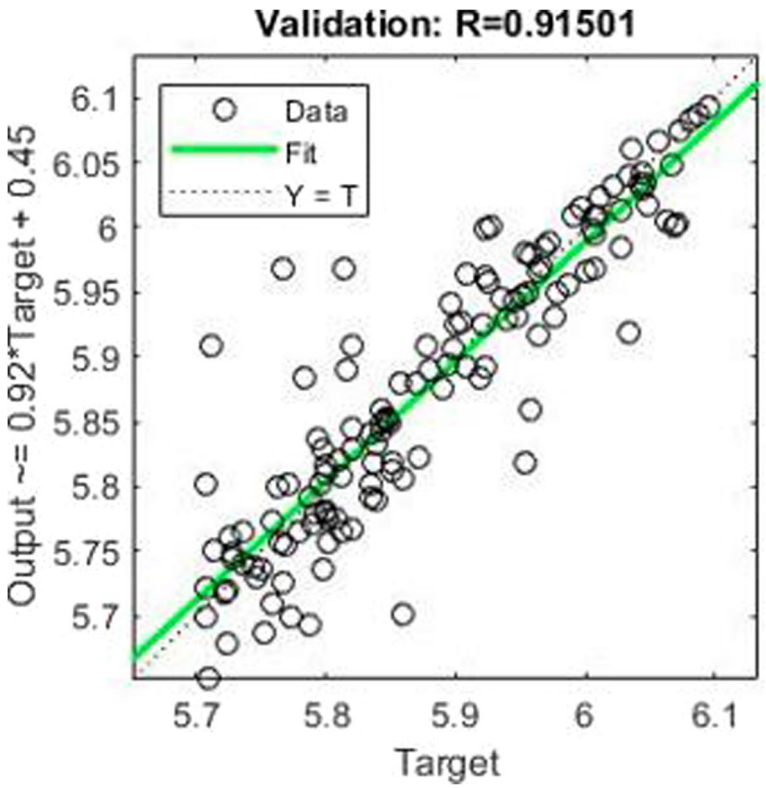

Fig. 5 *R* value (validation data)

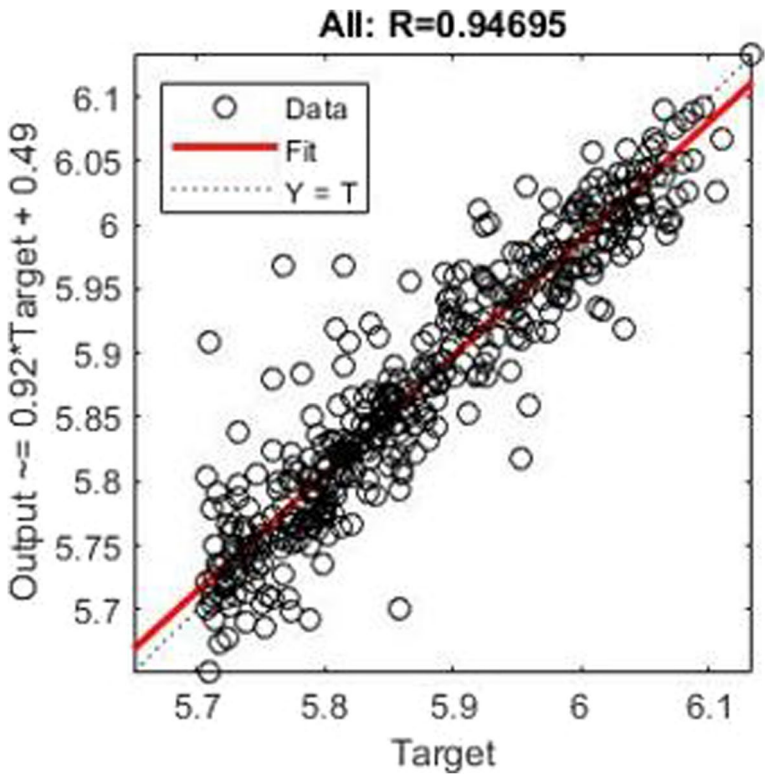

Fig. 6 *R* value (training and validation data)

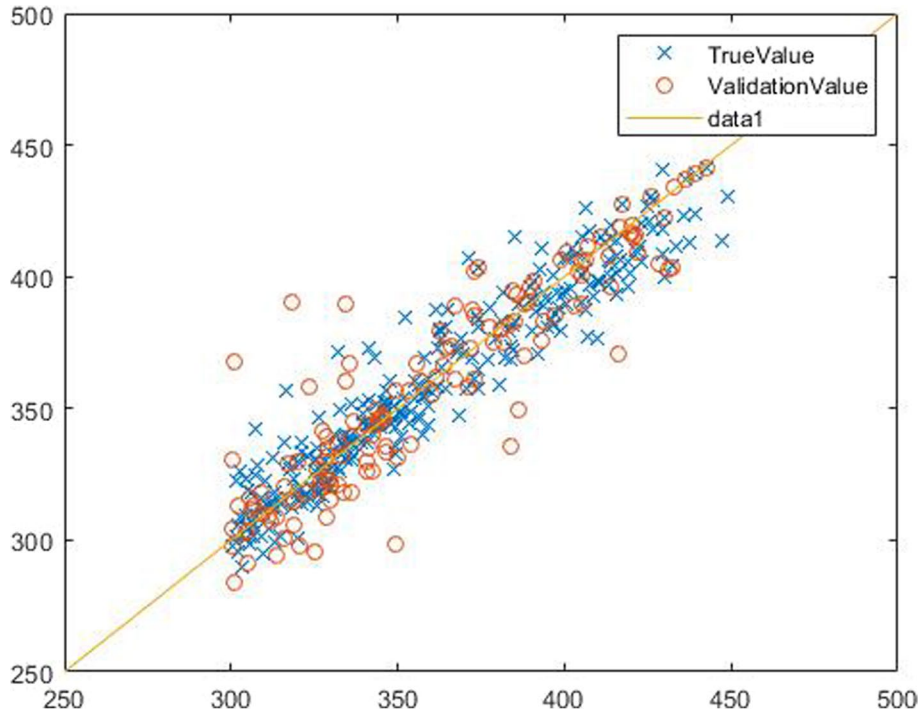

Fig. 7 Scatted data points

Table 3 Randomly generated input data (link lengths) and output (foot profile length) using ANN, GA, and regression approach

Test set	Input: link lengths (mm)							Output: foot profile length (mm)		
	L2	L3	L5	L7	Theta	L8	EQ	ANN	GA	Regression
1	219.86	288.2	101.78	286.83	0.6	271.45	2.17	248.63	63.35	237.77
2	147.51	178.59	274.52	369.57	0.93	459.17	164.2	148.06	494.46	468.59
3	303.93	271.66	183.9	411.41	0.18	523.31	79.24	507.30	302.33	393.68
4	177.78	250.89	309.06	443.45	1.95	515.18	− 22.81	338.94		437.30
5	136.01	149.47	269.63	453.94	1.35	477.2	116.67	309.47		433.46
6	193.38	302.27	304.93	484.46	3.21	404.16	136.41	885.40	229.02	238.09
7	110.09	243.76	291.64	288.9	1.5	256.46	39.77	268.05	229.023	324.79
8	106.51	208.6	170.46	393.84	1.89	347.66	96.35	369.82		289.46
9	213.26	194.78	307.52	313.96	1.53	284.39	− 6.67	436.84		375.71
10	237.69	169.01	283.99	342	4.07	445.86	5.61	202.78		523.75
11	110.2	294.08	196.9	339.71	2.68	433.62	129.92	262.24	212.66	368.31

Conclusions

Six different configurations of the 8-link planar Desai mechanism [22] were studied and found that the second configuration gives a bell-shaped foot profile for better walking stability. The second configuration is further studied by optimising the link dimensions using three different approaches such as mathematical model, regression, and ANN approach to obtain the optimum foot profile length of the walking robot.

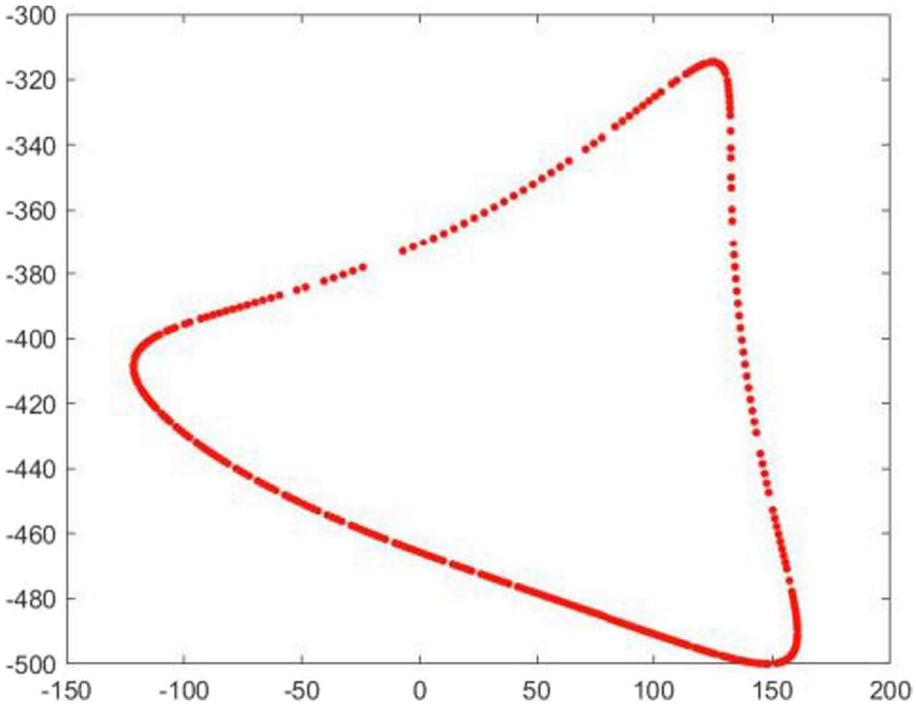

Fig. 8 Test set 1

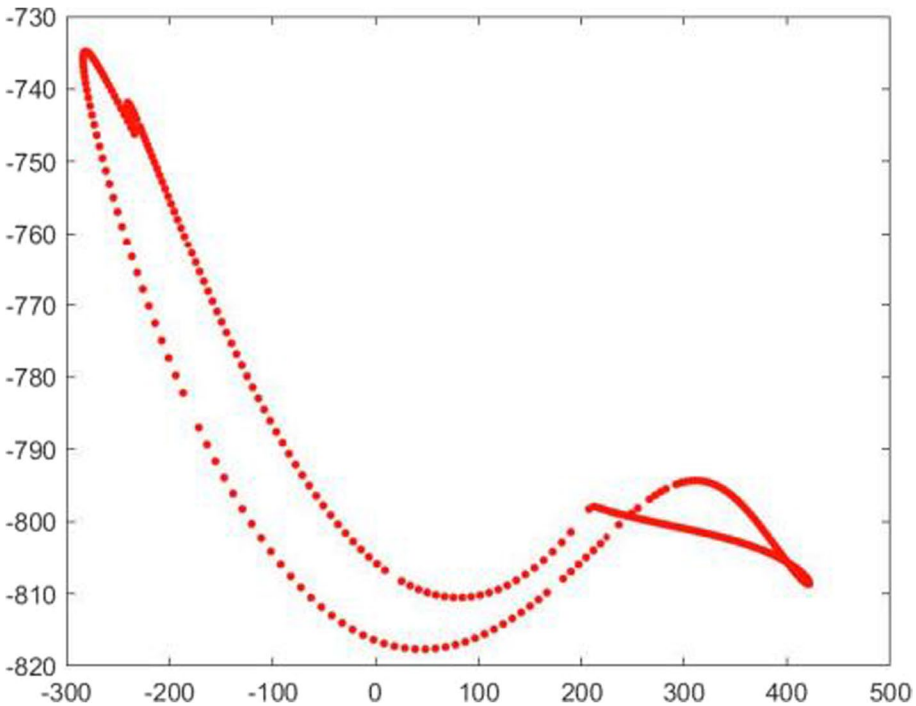

Fig. 9 Test set 2

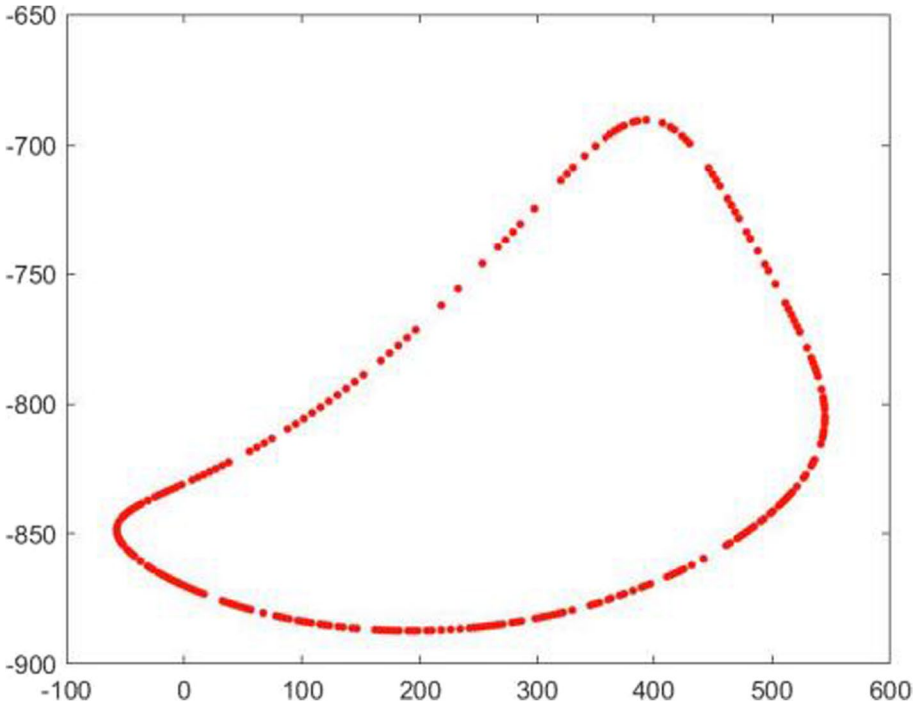

Fig. 10 Test set 3

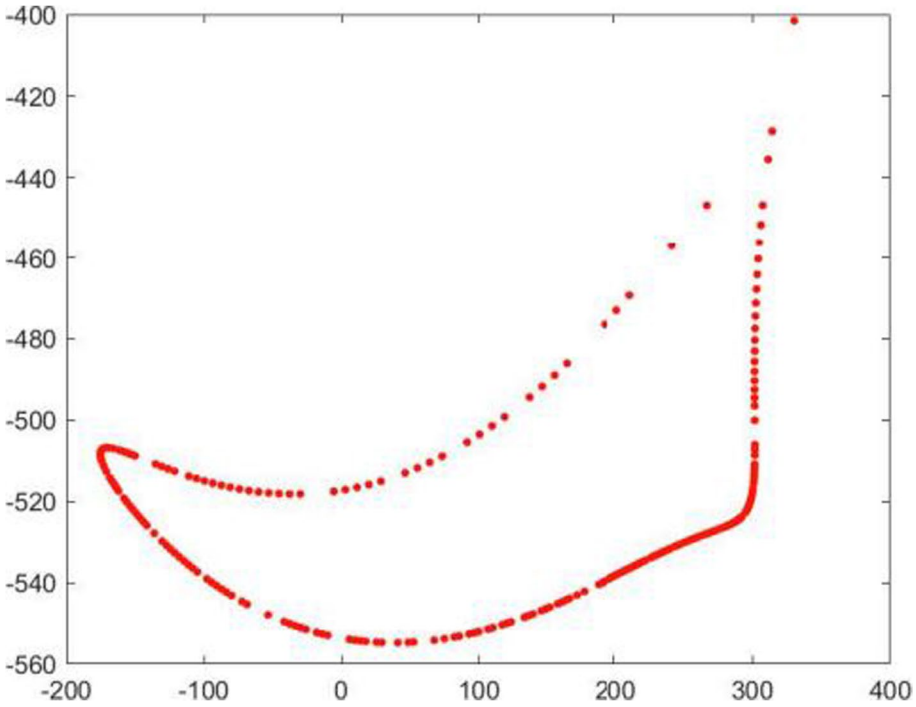

Fig. 11 Test set 6

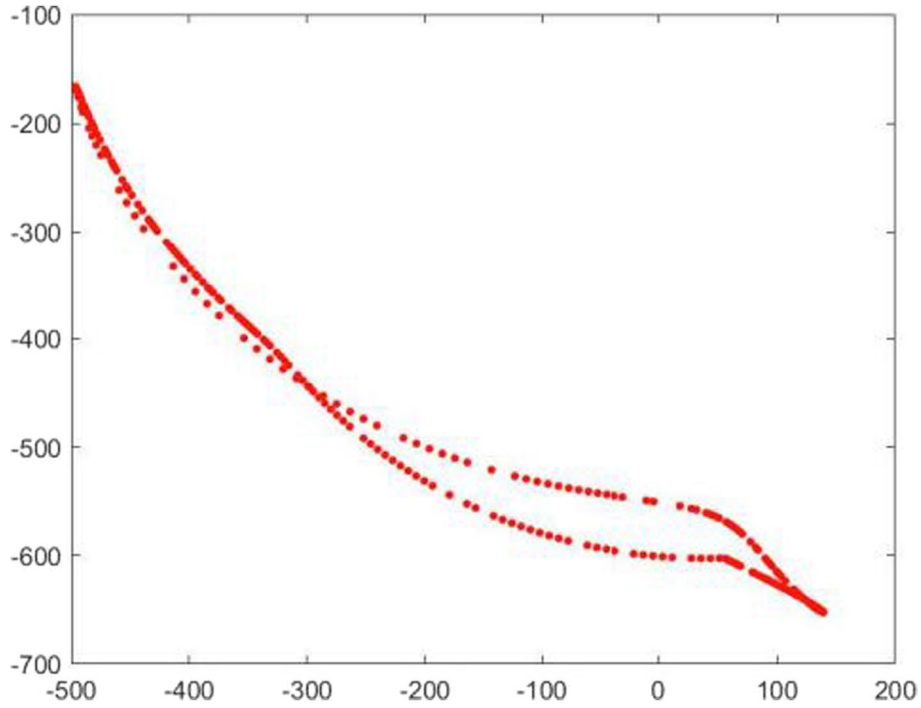

Fig. 12 Test set 7

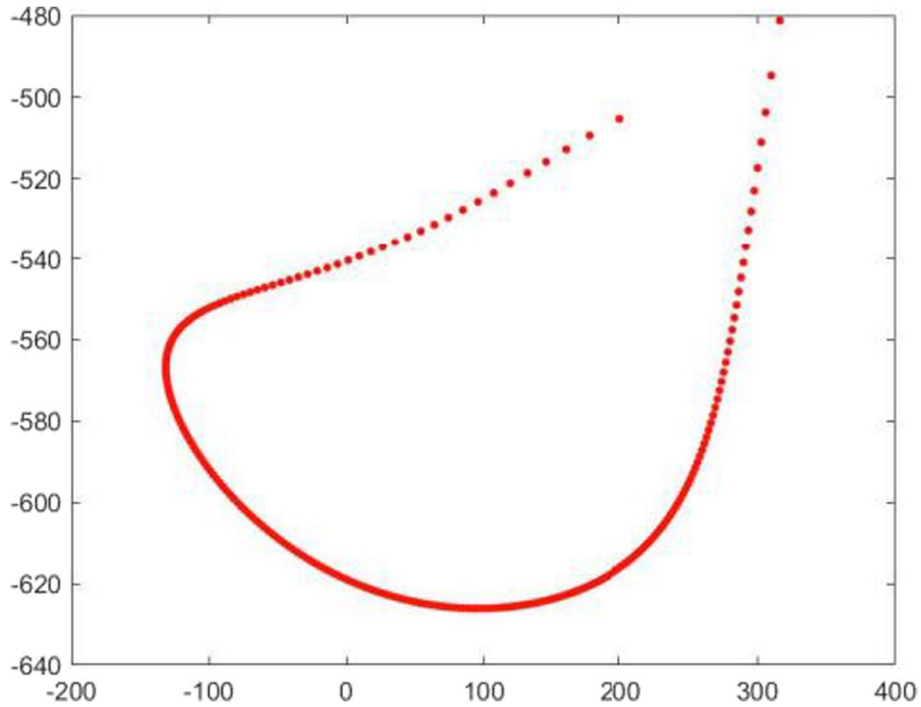

Fig. 13 Test set 11

The results of the three approaches used in this study are summarized below:

A mathematical model approach generates the output of foot profile lengths. In this approach, five different sample sizes were used, viz., 100, 200, 300, 400, and 500. The link

Table 4 Foot profile length and comparison of different test sets

Test set	Foot profile length in mm			Difference in %		
	ANN	GA	Regression	ANN and GA	ANN and regression	GA and regression
1	248.63	63.35	237.77	74.52	4.37	− 275.33
2	148.06	494.46	468.59	− 233.97	− 216.49	5.23
3	507.30	302.33	393.68	40.40	22.40	− 30.22
4	338.94	–	437.30	–	− 29.02	-
5	309.47	–	433.46	–	− 40.07	-
6	885.40	229.02	238.09	74.13	73.11	− 3.96
7	268.05	229.02	324.79	14.56	− 21.17	− 41.81
8	369.82	–	289.46	–	21.73	–
9	436.84	–	375.71	–	14.00	–
10	202.78	–	523.75	–	− 158.29	–
11	262.24	212.66	368.31	18.91	− 40.45	− 73.19

Table 5 Regression analysis

Predictor	Coefficient	Standard error coefficient	*T* (coefficient/standard error coefficient)	*P* value (Probability Score)
Constant	425.38	34.44	12.35	0
L2	-0.03818	0.06998	-0.55	0.586
L3	-0.7487	0.1274	-5.87	0
L5	0.37142	0.0546	6.8	0
L7	-0.9461	0.2456	-3.85	0
Theta	4.076	1.35	3.02	0.003
L8	0.9609	0.2336	4.11	0
TZ	-0.1175	0.1301	-0.9	0.367

S (standard error of regression) = 37.8467

R-squared (statistical measure of fit) = 17.9%

R-squared (adjusts for predictor) = 16.8%

Table 6 Analysis of variance

Source	DF (degrees of freedom)	SS (sum of squares)	MS (mean squares)	*F**	*P* value**
Regression	7	170,626	24,375	17.02	0
Residual error	548	784,938	1432		
Total	555	955,565			
Regression	7	170,626	24,375		
Total	555	955,565			

P Value** = Probability that measures the evidence

lengths followed a bell-shaped normal distribution curve indicating satisfactory output data.

A regression model is fitted for 500 samples. The *P* value observed for the link L_2 and EQ, which is more than the significance value, indicates no evidence against the null

Table 7 Minimum and maximum length of links in mm (randomly generated data for the test)

	L2	L3	L5	L7	Theta	L8	EQ
Min	106.5	146.28	100	285.76	0.1	256.08	-24.84
Max	321.62	304.51	321.94	491.63	4.10	535.49	166.26

hypothesis as shown in Tables 5 and 6. The *P* value for other links is statistically significant with the foot profile length.

The ANN model was designed to optimize the foot profile for the 8-link planar mechanism. The ANN model developed for various neurons in the hidden layer found that 18 neurons yield optimum results. Weights and bias are also determined to predict the results efficiently.

Test sets were randomly generated with the maximum and minimum values as shown in Table 7 for all three approaches and the link lengths were tested. Comparisons were made for foot profile length obtained through a mathematical model, regression model, and ANN.

The maximum difference of 19% in the foot profile is observed for ANN and the mathematical model. ANN and regression model show a maximum difference of 22.4% in the foot profile of the mechanism. The mathematical and regression approach shows a maximum of 5.23% difference in the result obtained.

In the future, the research focus will be to model the remaining configurations in [22] using GA, ANN, and Regression approaches. Simscape Multibody analysis of MATLAB software will be used to measure displacement, velocity, and acceleration of all the joints in the walking leg.

Acknowledgements
The authors acknowledge the organization for supporting this research work.

Authors' contributions
RBV developed the concept, methodology, and software codes for the research work, original draft, review, and editing. ARA performed the validation, and analysis of the work, original draft, review, and editing. JSS arranged the resources and simulation, prepared a draft manuscript, and reviewed and edited the manuscript. All authors read and approved the final manuscript.

Funding
Not applicable.

Availability of data and materials
The study data of this work can be shared upon request.

Declarations

Competing interests
The authors declare that they have no competing interests.

Received: 27 June 2023 Accepted: 29 September 2023
Published online: 16 October 2023

References

1. Max-Planck-Gesellschaft. Walking robot switches gaits autonomously and flexibly, 2010, https://www.sciencedaily.com/releases/2010/01/100117150824.htm. Accessed: 02 April 2023
2. Kousik S, Rahul S, Annigeri A R, Praveenkumar U B & Bharath M N. Performance analysis of quadruped robot designed with Desai's walking leg mechanism. Australian Journal of Mechanical Engineering, 2022; 1–14. https://doi.org/10.1080/14484846.2022.2087585

3. Oh SE, Choi A, Mun JH (2013) Prediction of ground reaction forces during gait based on kinematics and a neural network model. J Biomech 46:2372–2380. https://doi.org/10.1016/j.jbiomech.2013.07.036
4. Kahraman C, Deveci M, Boltürk E, Türk S (2020) Fuzzy controlled humanoid robots: A literature review. Robot Auton Syst 134:103643. https://doi.org/10.1016/j.robot.2020.103643
5. Woodford GW, du Plessis MC (2021) Bootstrapped neuro-simulation for complex robots. Robot Auton Syst 136:103708. https://doi.org/10.1016/j.robot.2020.103708
6. Kessis J. J., Rambaut J. P., Penne J., Wood R. and Mattar N. Hexapod walking robots with artificial intelligence capabilities. In Theory and Practice of Robots and Manipulators, 395–401, 1985, Springer, Boston, MA
7. Chau T (2001) A review of analytical techniques for gait data. Part 1: fuzzy, statistical and fractal methods. Gait Posture. 13:49–66. https://doi.org/10.1016/S0966-6362(00)00094-1
8. Chau T (2001) A review of analytical techniques for gait data Part 2: neural network and wavelet methods. Gait Posture 13:102–120. https://doi.org/10.1016/S0966-6362(00)00095-3
9. Mouloodi S, Rahmanpanah H, Gohari S, Burvill C, Tse KM, Davies HM (2021) What can artificial intelligence and machine learning tell us? A review of applications to equine biomechanical research. J Mech Behav Biomed Mater. 123:104728. https://doi.org/10.1016/j.jmbbm.2021.104728
10. Taha Z, Brown R, Wright D (1996) Realistic animation of human figures using artificial neural networks. Med Eng Phys 18(8):662–669. https://doi.org/10.1016/S1350-4533(96)00016-1
11. Abdolrasol MG, Hussain SM, Ustun TS, Sarker MR, Hannan MA, Mohamed R, Ali JA, Mekhilef S, Milad A (2021) Artificial neural networks based optimization techniques: a review. Electronics. 10:2689. https://doi.org/10.3390/electronics10212689
12. Di Gregorio R, Vocenas L (2021) Identification of Gait-Cycle Phases for Prosthesis Control. Biomimetics 6(2):22. https://doi.org/10.3390/biomimetics6020022
13. You Y, Xin S, Zhou C. and Tsagarakis N. Straight leg walking strategy for torque-controlled humanoid robots. Proceedings of IEEE International Conference on Robotics and Biomimetics (ROBIO), 2016, Qingdao, China, 2014–2019. https://doi.org/10.1109/ROBIO.2016.7866625
14. Kim BH (2013) Work analysis of compliant leg mechanisms for bipedal walking robots. Int J Adv Rob Syst 10(9):334. https://doi.org/10.5772/56926
15. Terefe TO, Lemu HG, Tuli TB (2019) Kinematic modeling and analysis of a walking machine (robot) leg mechanism on a rough terrain. Adv Sci Technol Res J. 13:43–53. https://doi.org/10.12913/22998624/109792
16. Gheorghita V. and Gheorghita C. Applying regression analysis to optimize the length of components of a six bar mechanism, IOP Conference Series: Materials Science and Engineering, 2018, 400, 042024. https://doi.org/10.1088/1757-899x/400/4/042024
17. Tavakoli NH, Zohour H (2005) Optimal synthesis of planar and spatial mechanism for path generation using regression deviation. Scientia Iranica. 12(2):190–198. https://www.sid.ir/en/journal/ViewPaper.aspx?id=35034
18. Nguyen V, Marvel JA (2022) Modeling of Industrial Robot Kinematics Using a Hybrid Analytical and Statistical Approach. ASME J Mech Robot 14:051009. https://doi.org/10.1115/1.4053734
19. Ruiz DV, Magluta C, Roitman N (2022) Experimental verification of biomechanical model of bipedal walking to simulate vertical loads induced by humans. Mech Syst Signal Process 167:108513. https://doi.org/10.1016/j.ymssp.2021.108513
20. Zhang Y, Arakelian V (2021) Design and synthesis of single-actuator walking robots via coupling of linkages. Front Mech Eng 6:609340. https://doi.org/10.3389/fmech.2020.609340
21. Biswal P, Mohanty PK (2021) Development of quadruped walking robots: a review. Ain Shams Eng J 12:2017–2031. https://doi.org/10.1016/j.asej.2020.11.005
22. Desai SG, Annigeri AR, TimmanaGouda A (2019) Analysis of a new single degree-of-freedom eight link leg mechanism for walking machine. Mech Mach Theory 140:747–764. https://doi.org/10.1016/j.mechmachtheory.2019.06.002
23. Safartoobi M, Dardel M, Daniali HM (2021) Gait cycles of passive walking biped robot model with flexible legs. Mech Mach Theory 159:104292. https://doi.org/10.1016/j.mechmachtheory.2021.104292
24. Raghavendra BV, Annigeri AR (2021) Optimal synthesis of planar eight-link walking leg mechanism using genetic algorithm. Int J Model Ident Control 38:152–164. https://doi.org/10.1504/IJMIC.2021.122498
25. Paulo Davim J. Design of Experiments in Production Engineering. Springer, 2016, ISBN: 978–3–319–23838–8, https://doi.org/10.1007/978-3-319-23838-8
26. Paulo Davim J. Computational methods and production engineering. Elsevier, 2017, ISBN:9780857094810
27. Paulo Davim J. Statistical and Computational Techniques in Manufacturing. Springer, 2012, ISBN: 978–3–642–25859–6, https://doi.org/10.1007/978-3-642-25859-6
28. Paulo Davim J. Mechanical and industrial engineering historical aspects and future directions, Springer, 2022, ISBN: 978–3–030–90487–6, https://doi.org/10.1007/978-3-030-90487-6
29. Abdelwahab SAM, Hamada AM, Abdellatif WS (2020) Comparative analysis of the modified perturb & observe with different MPPT techniques for PV grid connected systems. Intern J Renew Energy Res 10(1):55–164
30. Elbaset, A. A., Abdelwahab, S. A. M., Ibrahim, H. A., Eid, M. A. E. (2019). Performance analysis of photovoltaic systems with energy storage systems. Springer International Publishing.
31. S. S. Dessouky, A. A. Elbaset, A. H. K. Alaboudy, H. A. Ibrahim and S. A. M. Abdelwahab, Performance improvement of a PV-powered induction-motor-driven water pumping system, 2016 Eighteenth International Middle East Power Systems Conference (MEPCON), Cairo, Egypt, 2016, pp. 373-379, https://doi.org/10.1109/MEPCON.2016.7836918
32. Elnozahy A, Yousef AM, Ghoneim SSM et al (2021) Optimal Economic and Environmental Indices for Hybrid PV/Wind-Based Battery Storage System. J Electr Eng Technol 16:2847–2862. https://doi.org/10.1007/s42835-021-00810-9
33. Yousef, A. M., Ebeed, M., Abo-Elyousr, F. K., Elnozohy, A., Mohamed, M., & Abdelwahab, S. M. (2020). Optimization of PID controller for hybrid renewable energy system using adaptive sine cosine algorithm. Intern J Renew Energy Res-IJRER, 670–677. https://doi.org/10.20508/ijrer.v10i2.10685.g7938

34. Yousef AM, Abo-Elyousr FK, Elnozohy A, Mohamed M, Abdelwahab SAM (2020) Fractional order PI control in hybrid renewable power generation system to three phase grid connection. Intern J Electr Eng Inform 12(3):470–493. https://doi.org/10.15676/ijeei.2020.12.3.5
35. Babes B, Hamouda N, Albalawi F, Aissa O, Ghoneim SS, Abdelwahab SAM (2022) Experimental investigation of an adaptive fuzzy-neural fast terminal synergetic controller for buck DC/DC converters. Sustainability 14(13):7967. https://doi.org/10.3390/su14137967
36. Oubelaid A, Albalawi F, Rekioua T, Ghoneim SSM, Taib N, Abdelwahab SAM (2022) Intelligent torque allocation based coordinated switching strategy for comfort enhancement of hybrid electric vehicles. IEEE Access 10:58097–58115. https://doi.org/10.1109/ACCESS.2022.3178956
37. Bahaa Saleh, Ali M. Yousef, Farag K. Abo-Elyousr, Moayed Mohamed, Saad A. Mohamed Abdelwahab & Ahmed Elnozahy (2022) Performance analysis of maximum power point tracking for two techniques with direct control of photovoltaic grid -connected systems. Energy Sources Part A Recovery Util Environ Eff 44(1):413–434. https://doi.org/10.1080/15567036.2021.1898496
38. Elnozahy A, Yousef AM, Abo-Elyousr FK, Mohamed M, Abdelwahab SAM (2021) Performance improvement of hybrid renewable energy sources connected to the grid using artificial neural network and sliding mode control. J Power Electron 21:1166–1179. https://doi.org/10.1007/s43236-021-00242-8

Publisher's Note